A DSP Controlled Adaptive Feedforward Amplifier Linearizer

Stephen J. Grant
James K. Cavers
School of Engineering Science, Simon Fraser University
Paul A. Goud
Dept. of Electrical Engineering, University of Alberta

***Abstract*—Currently, the only available wideband (multiple MHz) amplifier linearization method is feedforward. Feedforward, though, requires automatic adaptation of key parameters for reliable distortion cancellation as operating conditions vary. With a novel and appropriate use of DSP, we have implemented a feedforward linearizer with adaptation driven by easily computed gradient signals. This overcomes the difficulties, such as DC offsets at the output of analog mixers and masking of weak signals by stronger ones, that slow and/or cause incorrect convergence of many previously reported implementations. The result is an average of 40 dB reduction in intermodulation spectra over a wide bandwidth, with extremely fast tracking.**

INTRODUCTION

RF power amplifiers (PAs) generate intermodulation (IM) distortion if they carry linear modulation or several frequency channels at once. Since IM distortion appears as interference in other channels, amplifier linearization is an essential element of a PCS. Of the known linearization strategies [1-5], only feedforward can provide good IM reduction over an operating bandwidth of tens of MHz, and it does so through its use of inherently wideband analog technology. The feedforward method, though, is very sensitive to parameter changes due to varying operating conditions such as input power level, supply voltage and temperature. Adaptation is thus essential.

Two significant problems have compromised many previous adaptation structures, e.g. [6]. One of them is the generation of a gradient signal by bandpass correlation of RF signals to produce a DC result. With analog mixing of the RF signals, any DC offset in the result causes convergence to incorrect parameter values. A second problem is masking of weak signals by strong ones in one gradient calculation, causing extremely slow convergence. This paper demonstrates a novel and appropriate use of DSP to solve both problems regardless of the bandwidth of the carried signals.

THE FEEDFORWARD STRUCTURE

Basic Feedforward Operation

Fig. 1 shows that a feedforward linearizer consists of cascaded signal cancellation and error cancellation circuits. In the signal cancellation circuit, the RF input signal $v_m(t)$ is split into amplification and reference branches. In the amplification branch, the signal is attenuated and shifted in phase by controllable values, and then fed to the PA. The PA output signal $v_a(t)$ is sampled with a coupler and attenuated to reduce its level to that of the reference signal where the two are combined in antiphase. With appropriate selection of the controllable attenuation and phase shift, the reference signal is canceled, leaving an error signal $v_e(t)$ which is an attenuated version of the IMD generated by the PA. In the error cancellation circuit, the error signal is attenuated and shifted in phase, again by a controllable value, and amplified in an error amplifier. When it is injected back into the main signal path, the IMD is canceled, leaving only a linearly amplified version $v_o(t)$ of the RF input. Delay lines in each circuit are necessary to compensate for the group delay of the PA and the error amplifier.

The crux of the operation of the adaptive feedforward linearizer is proper adjustment of the attenuation and phase parameters in each circuit and selection of a highly linear error amplifier so that no additional (uncorrectable) IMD is introduced in the linearizer output. These issues will be discussed in more detail in the subsequent sections.

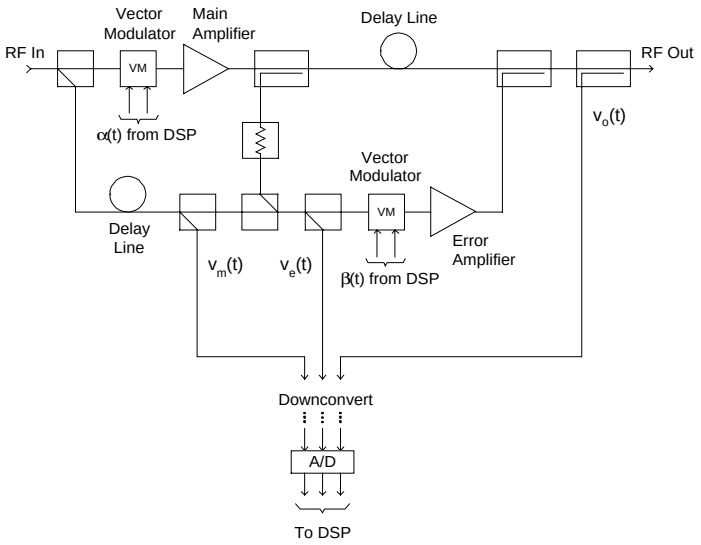

Fig. 1. Adaptive feedforward amplifier linearizer

Principles of Adaptation

A simplified baseband equivalent (Fig. 2) of the feedforward linearizer is useful for analyzing adaptation. Signals are replaced by their complex envelopes. Adaptive complex coefficients α and β represent the attenuation and

phase shift introduced in both the signal and error cancellation circuits respectively. The power amplifier is modeled as a memoryless nonlinearity whose AM/AM and AM/PM conversion is summarized by its complex voltage gain $G(x)$, where x denotes instantaneous power. The PA output $v_a(t)$ is therefore

$$v_a(t) = \alpha v_m(t) G\left(\left|\alpha v_m(t)\right|^2\right) \tag{1}$$

which consists of a linearly amplified term $c_0 \alpha v_m(t)$ and a distortion term $v_d(t)$. The complex coefficient c_0 is the first coefficient of the power series expansion of the nonlinear function $G(x)$. For this analysis, we also assume that delay matching is accurate and that the error amplifier is perfectly linear.

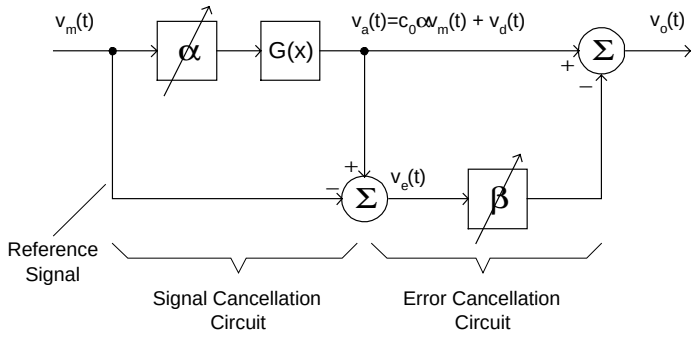

Fig. 2. Complex baseband equivalent model

A detailed analysis of gradient based adaptation without pilot signals, including accuracy requirements and convergence time and jitter, is contained in [7], and is summarized here. Adaptation of α, based on the linear estimation of $v_a(t)$ with basis $v_m(t)$, is designed to minimize P_e, the average power of the error signal. When P_e is minimized, the error signal is simply the IMD introduced by the PA, $v_d(t)$, with the reference signal completely canceled. If the coefficient α were placed in the lower (reference) branch, making $v_e(t) = v_a(t) - \alpha v_m(t)$, then P_e would be a quadratic function of α with a well defined minimum. A suitable gradient signal would be the covariance of the estimation error and the reference signal, for which a noisy, but unbiased estimate is

$$D_\alpha(t) = v_e(t) v_m^*(t) \tag{2}$$

When α is adjusted properly, $E[D_\alpha(t)] = 0$, since the optimal linear estimate occurs when the estimation error and the basis of the estimate are uncorrelated. This suggests the following algorithm for the adaptation of α implemented as a first order circuit

$$\alpha(t) = K_\alpha \int_0^t D_\alpha(\tau) d\tau \tag{3}$$

where K_α controls the time constant of the adaptation. For our placement of α in the upper (amplification) branch instead, it is shown in [8] that an identical gradient signal and adaptation algorithm cause convergence to the optimum value, despite the interaction of the coefficient and the PA.

The adaptation of β proceeds in a similar manner except that the basis of the estimate of $v_a(t)$ is $v_e(t)$ and the estimation error is $v_o(t)$. The gradient signal for the adjustment of β is

$$D_\beta(t) = v_o(t) v_e^*(t) \tag{4}$$

and the algorithm for adaptation is

$$\beta(t) = K_\beta \int_0^t D_\beta(\tau) d\tau \tag{5}$$

where K_β is analogous to K_α.

Problems in Adaptation

There are two main problems in conventional feedforward adaptation. The first appears if the gradients (2) and (4) are implemented by bandpass correlation of the corresponding RF signals to produce a lowpass result. DC offsets and $1/f$ noise in the mixers cause convergence to incorrect values, weakening the degree of IM suppression. The second is that the gradient (4) relies on mixing of $v_e(t)$ with the weak IM component in $v_a(t)$. The much stronger signal component in $v_a(t)$ acts as noise, forcing a very long time constant and thus slow convergence. We have solved both problems—the first, by use of DSP to perform correlation, and the second, by use of a filter to suppress the desired signal component in $v_o(t)$.

IMPLEMENTATION

Equation (3) is implemented in DSP by use of the familiar LMS algorithm

$$\alpha(n) = \alpha(n-1) + \delta D_\alpha(n) \tag{6}$$

where the parameter δ is the step size. Equation (5) is implemented in an analogous manner. Fig. 1 shows the points in the feedforward circuit where the appropriate RF signals are split to enable downconversion and sampling before recovering the required complex envelopes in DSP.

The real and imaginary components of $\alpha(n)$ and $\beta(n)$ are used directly as the control signals for the vector modulators (VMs) in the signal and error cancellation circuits which realize the required attenuation and phase shift. Both VMs have highly linear RF input/output characteristics—an important property, especially in the error cancellation circuit. The attenuation and phase shift provided by the VMs varies monotonically with the control voltages; this ensures convergence of α and β to the correct values.

For wide bandwidth operation, the gradient signals for the adaptation of α and β cannot be computed in one step due to limited sampling rates available for DSP. Thus, the gradient computations must be performed in subbands spanning selected spectral regions of the signals and the result from each subband summed. This method is validated by replacing the time domain integrals in equations (3) and (5) with the corresponding frequency domain integrals using Parseval's theorem. Various subbands may be selected by employing a

two- or three-step downconversion process in which the frequency of the first oscillator controls which portion of the signal is placed in the narrow window of the first IF filter; the second and/or third oscillators remain fixed.

The main amplifier in Fig. 1 is a 5 Watt, 815 MHz, class AB PA driven by a narrowband π/4-DQPSK modulated signal centred about 815 MHz. The data signal employs root raised cosine pulse shaping with 35% rolloff at a symbol rate of 20 ksym/s. A narrowband, rather than wideband, data signal is used so that the gradient computation may be performed in only one step, rather than several steps as described above. The error amplifier is a 5 W class A amplifier which operates with sufficient backoff to ensure linear operation.

Since $v_m(t)$, $v_e(t)$, and $v_o(t)$ are bandpass signals, the DC offsets generated by the mixers in the downconversion process can be avoided by centering the signals about an IF low enough to be sampled, but high enough to ensure no spectral occupancy at DC, and then accurately recovering the corresponding complex envelopes in DSP. In the present implementation, this is achieved using a sampling rate of f_s = 150 kHz and an IF of $f_s/4$. Note that the same oscillators are used to downconvert each of the three signals $v_m(t)$, $v_e(t)$, and $v_o(t)$.

For the adaptation of α, the complex envelopes of $v_m(t)$ and $v_e(t)$ are recovered using complex bandpass FIR filters of length 16 centred about $f_s/4$ which provide 40 dB image suppression. The filter stopband extends from $f_s/2$ to f_s. The high stopband attenuation is achieved with a short filter by allowing the transition bandwidth to be wide. This is acceptable, since the spectral region of interest for the correlation of $v_m(t)$ and $v_e(t)$ is that occupied by the reference signal only. No sample-by-sample derotation of the filter outputs is necessary since the constellation rotations are canceled by the complex conjugate multiplication performed in the gradient calculation. For the same reason, any frequency offset in the downconverted signals from the IF of $f_s/4$ is canceled.

The adaptation of β is implemented in a similar fashion with one notable difference. The masking problem is solved by modifying the filter used to recover the complex envelope of $v_o(t)$ by introducing a notch in the bandpass frequency response to suppress the signal component. The resulting filter is a complex bandstop FIR filter of length 53 which provides 60 dB attenuation of the signal component and 40 dB image suppression. In contrast to the filters used for the adaptation of α, the transition bandwidths for the bandstop filter must be narrow, since the spectral region of interest for the correlation of $v_o(t)$ and $v_e(t)$ is that occupied by the distortion outside the band of the desired signal. A similar complex bandpass filter to those used for the adaptation of α is used for $v_e(t)$, except its length is 53 to match the length of the bandstop filter used for $v_o(t)$, and to ensure narrow transition bandwidths.

To reduce development time, the DSP used for the adaptation of α and β is TI's TMS320C30 floating point processor. Due to processing power constraints, the filter outputs for the adaptation of α and β are decimated by a factor equal to the corresponding filter lengths—16 for α and 53 for β. The effect of this simplification is a longer adaptation time constant as shown in the following section. Note that the choice of the filter lengths for the decimation factors simplifies the DSP code; smaller factors could be used. Moreover, with a slightly faster DSP, decimation would not be necessary at all.

RESULTS

The convergence behavior of α and β is illustrated in plots of the control voltages for the vector modulators in the signal and error cancellation circuits (Figs. 3 & 4). Starting from zero, the initial convergence time of α is less than 0.3 sec, and the reconvergence time due to a 6 dB drop in input power at time t ≈ 5.55 is less than 50 msec. As can be seen in Fig. 4, β is not affected by the step change in input power, thus no loss in IM suppression occurs during this time. The initial convergence time of β, approximately 2.5 sec, is longer than that for α, but once converged, β does not have to adapt to changes in operating conditions as quickly as α. Note that because of the decimation involved in the DSP implementation of the LMS algorithm discussed previously, the convergence time for α is slowed by a factor of 16, and for β by a factor of 53. Thus, if no decimation is required, the initial convergence times of α and β would drop to approximately 20 and 50 msec respectively, and the reconvergence time of α would drop to approximately 3 msec.

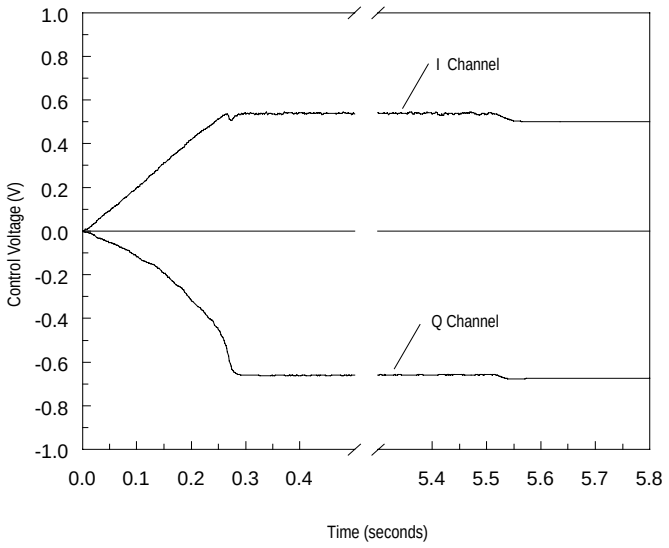

Fig. 3. Convergence of α

Fig. 5 illustrates approximately a 30 dB reduction in intermodulation spectra achieved by the adaptive feedforward linearizer for an input narrowband data signal. The resulting linearizer output spectrum is virtually identical to the spectrum of the input signal. The corresponding PA output power is +34 dBm, which is approximately 3 dB below the amplifier's output 1 dB compression point. Note that the plot of the output spectrum without linearization is obtained by allowing α to

converge to its optimal value which determines the PA operating point, and then disconnecting the error cancellation circuit from the output coupler so that the amplifier distortion is not suppressed.

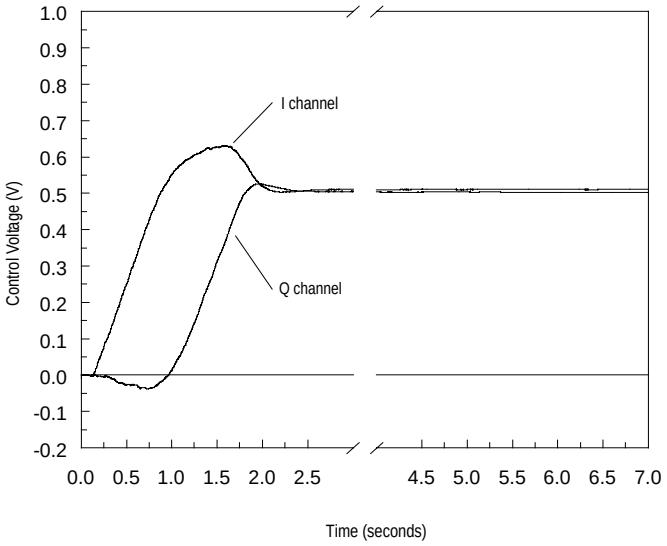

Fig. 4. Convergence of β

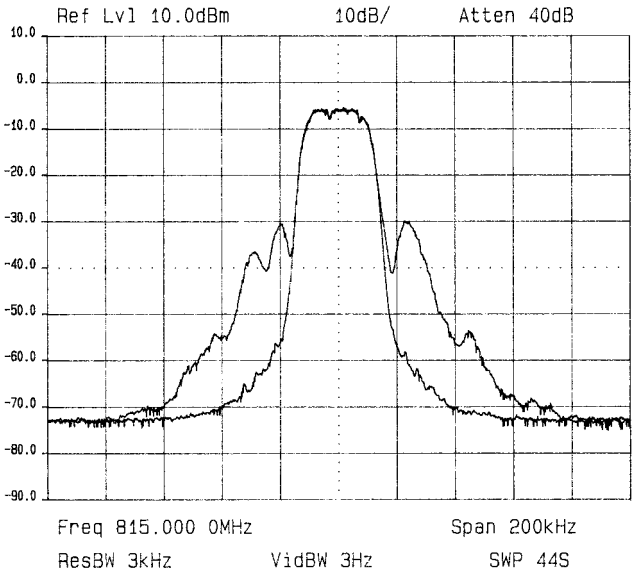

Fig. 5. Output spectra for power amplifier with and without linearization for a narrowband data signal

Fig. 6 demonstrates that the feedforward linearizer is capable of wide bandwidth operation. A single tone at 812.5 MHz (2.5 MHz offset from band center) is combined with the narrowband data signal at the linearizer input. Note that the adaptation algorithm is still based on the narrowband data signal centred at 815 MHz as before; in effect, the added tone is transparent. At the output of the power amplifier, intermodulation products appearing at multiples of 2.5 MHz offset from band center are indeed canceled by up to 40 dB evident from the residual IM product at 817.5 MHz. Further tests show 40 dB cancellation for tone offsets up to 3.5 MHz, thus the effective bandwidth is double this, i.e. 7 MHz. The effective bandwidth for 30 dB cancellation is measured as 10 MHz.

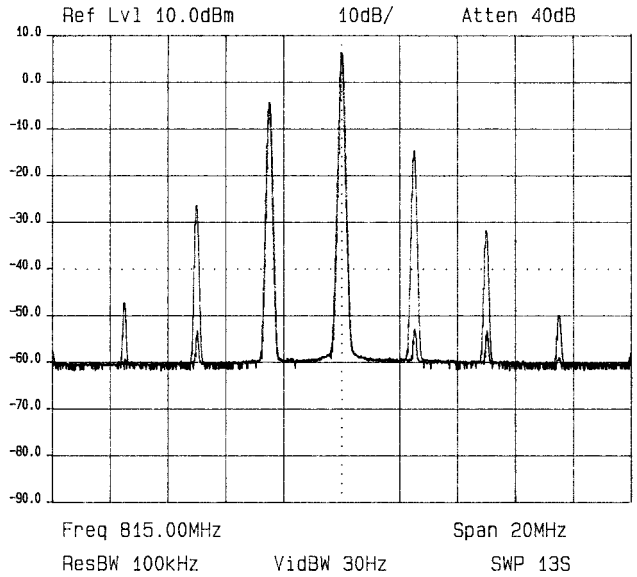

Fig. 6. Output spectra for narrowband data signal plus tone

CONCLUSIONS

We have implemented a gradient driven adaptive feedforward amplifier linearizer with a novel use of DSP that overcomes the problems of mixer DC offsets and masking of strong signals by weaker ones that compromise other previously proposed analog implementations. The result is a 40 dB reduction in IM spectra over a bandwidth of at least 7 MHz with extremely fast tracking. Initial convergence of the adaptation algorithm occurs in approximately 50 msec, and following a sudden reduction of signal level by 6 dB, it reconverges in approximately 3 msec, during which time there is no loss of IM suppression.

REFERENCES

[1] Y. Akaiwa and Y. Nagata, "Highly Efficient Digital Mobile Communication with a Linear Modulation Method," *IEEE JSAC*, vol. SAC 5, no. 5, pp. 890-895, June 1987.

[2] Y. Nagata, "Linear Amplification Technique for Digital Mobile Communications," Proc IEEE Vehicular Tech. Conf., pp. 159-164, May 1989.

[3] H. Seidel, "A Microwave Feedforward Experiment," BSTJ, vol. 50, no. 9, pp. 2879-2918, November 1971.

[4] S. Narahashi and T. Nojima, "Extremely Low-Distortion Multi-Carrier Amplifier - Self Adjusting Feed-Forward (SAFF) Amplifier," IEEE ICC, pp. 1485-1490, 1991.

[5] J.K. Cavers, "Adaptive Feedforward Linearizer for RF Power Amplifiers," U.S. Patent 5,489,875, February 6, 1996.

[6] R.M. Bauman, “Adaptive feed-forward system,” U.S. Patent 4,389,618, June 21, 1983.
[7] J.K. Cavers, “Adaptation Behavior of a Feedforward Amplifier Linearizer,” IEEE Trans. Vehicular Tech., vol. 44, no. 1, pp. 31-40, February 1995.
[8] S.J. Grant, “A DSP Controlled Adaptive Feedforward Power Amplifier Linearizer,” M.A.Sc. Thesis, School of Engineering Science, Simon Fraser University, July 1996.